available at www.sciencedirect.com

ScienceDirect

journal homepage: www.elsevier.com/locate/biochempharm

Thermodynamics of A_{2B} adenosine receptor binding discriminates agonistic from antagonistic behaviour

Stefania Gessi [a], *Eleonora Fogli* [a], *Valeria Sacchetto* [a], *Katia Varani* [a], *Stefania Merighi* [a], *Edward Leung* [b], *Stephen Mac Lennan* [b], *Pier Andrea Borea* [a,*]

[a] *Department of Clinical and Experimental Medicine, Pharmacology Unit and Interdisciplinary Center for the Study of Inflammation, Ferrara, Italy*

[b] *King Pharmaceutical, Inc., Research and Development, Cary, NC, United States*

ARTICLE INFO

Article history:
Received 13 July 2007
Accepted 4 September 2007

Keywords:
Binding thermodynamics
Adenosine A_{2B} receptor
Enthalpy–entropy compensation
Agonist–antagonist discrimination
Binding mechanisms
Drug development

ABSTRACT

Thermodynamic parameters ΔG°, ΔH° and ΔS° of the binding equilibrium of 12 ligands (six agonists and six antagonists) to the A_{2B} adenosine receptor subtype have been determined by affinity measurements carried out on HEK 293 cells stably transfected with human A_{2B} adenosine receptors at six different temperatures (4, 10, 15, 20, 25, 30 °C) and van't Hoff plot analysis have been performed. Affinity constants were obtained from saturation experiments of [^{3}H]MRE 2029-F20 or by its displacement in inhibition assays for the other compounds. van't Hoff plots were essentially linear in the temperature range investigated, showing that the ΔC_p° of the binding equilibrium is nearly zero. Thermodynamic parameters are in the range $7 \leq \Delta H^\circ \leq 23$ kJ mol^{-1}and $123 \leq \Delta S^\circ \leq 219$ J K^{-1} mol^{-1} for agonists and $-40 \leq \Delta H^\circ \leq -20$ kJ mol^{-1} and $10 \leq \Delta S^\circ \leq 91$ J K^{-1} mol^{-1} for antagonists indicating that agonistic binding is always totally entropy-driven while antagonistic binding is enthalpy and entropy-driven. In the $-T\Delta S^\circ$ versus ΔH° plot the thermodynamic data are clearly arranged in separate clusters for agonists and antagonists, which, therefore, turn out to be thermodynamically discriminated.

* *Corresponding author at*: University of Ferrara, Department of Clinical and Experimental Medicine, Pharmacology Unit, Via Fossato di Mortara 17-19, 44100 Ferrara, Italy. Tel.: +39 0532 455214; fax: +39 0532 455205.
E-mail address: bpa@dns.unife.it (P.A. Borea).

Abbreviations: AB-MECA, 4-aminobenzyl-5′-*N*-methylcarboxamidoadenosine; CGS 21680, 2-[*p*-(carboxyethyl)-phenethylamino]-NECA; CGS 15943, 5-amino-9-chloro-2-(furyl)1,2,4-triazolo[1,5-c]quinazoline; CHA, N^6-cyclohexyladenosine; Cl-IB-MECA, N^6(3-iodobenzyl)2-chloroadenosine-5′*N*-methyluronamide; Compound 24, 1-deoxy-1-[6-{4-[(phenylcarbamoyl)-methoxy]phenylamino}-9H-purin-9-yl]-*N*-ethyl-β-D-ribofuranuronamide; Compound 34, 1-deoxy-1-[6-{4-[(4-*tert*-butyl-phenylcarbamoyl)-methoxyl-phenylamino}-9H-purin-9-yl]-*N*-ethyl-β-D-ribofuranuronamide; Compound 17b, *N*-[5-(2,6-dioxo-1,3-dipropyl-2,3,6,7-tetrahydro-1H-purin-8-yl)-1-methyl-1H-pyrazol-3-yl]-2-phenyl-acetamide; Compound 21b, 2-(4-benzyloxy-phenyl)-*N*-[5-(2,6-dioxo-1,3-dipropyl-2,3,6,7-tetrahydro-1H-purin-8yl)-1-methyl-1H-pyrazol-3-yl]-acetamide; CPA, N^6-cyclopentyladenosine; CPT, 8-cyclopentylxanthine; DPCPX, 1,3-dipropyl-8-cyclopentyl-xanthine; DPSPX, 1,3-dipropyl-8-sulfophenyl-xanthine; hHEK293-A_{2B}, HEK293 cells transfected with human A_{2B} adenosine receptor; IB-MECA, N^6-(3-iodobenzyl) adenosine-5′-*N*-methyluronamide; IBMX, 3-isobutyl-1-methylxanthine; MRE 2029-F20, *N*-benzo[1,3]dioxol-5-yl-2-[5-(1,3-dipropyl-2,6-dioxo-2,3,6,7-tetrahydro-1H-purin-8-yl)-1-methyl-1H-pyrazol-3-yl-oxy]-acetamide]; MRE 3008-F20, 5-*N*-(4-methoxyphenylcarbamoyl)-amino-8-propyl-2-(2-furyl)-pyrazolo[4,3e]-1,2,4triazolo[1,5c]pyrimidine; MRE 3020-F20, 5-*N*-(3-chlorophenylcarbamoyl)-amino-8-ethyl-2(2-furyl)pyrazolo[4,3e]1,2,4triazolo[1,5c]pyrimidine; MRE 3005-F20, 5-*N*-(4-methoxyphenylcarbamoyl)amino-8-phenyl-ethyl-2-(2-furyl)-pyrazolo-[4,3e]1,2,4-triazolo[1,5c]-pyrimidine; NECA, 5′-*N*-ethyl-carboxamidoadenosine; 8-PT, 8-phenyltheophylline; R-PIA, R(−)-N^6-(2-phenyl-isopropyl)adenosine; SCH 58261, 5-amino-7-(2-phenylethyl)-2-(2-furyl)-pyrazolo[4,3-*e*]-1,2,4-triazolo[1,5-c]-pyrimidine; SCH 63390, 5-amino-7-(3-phenylpropyl)-2-(2-furyl)-pyrazolo[4,3-e]-1,2,4-triazolo[1,5-c]pyrimidine; S-PIA, S(−)N^6-(2-phenyl-isopropyl)adenosine; ZM, 241385 (4-(2-[7-amino-2-(2-furyl)-[1,2,4]triazolo-[2,32][1,3,6]triazinyl-amino]ethyl)-phenol).

0006-2952/$ – see front matter
doi:10.1016/j.bcp.2007.09.003

1. Introduction

Thermodynamic studies of drug–receptor interactions have aroused increasing interest in recent years, due to the information that they can provide on molecular binding mechanisms. In fact, a simple determination of association binding constant make it possible to calculate the standard free energy $\Delta G^\circ = -RT \ln K_A$ ($T = 298.15$ K) of the binding equilibrium, but not its two components as defined by the Gibbs equation $\Delta G^\circ = \Delta H^\circ - T\Delta S^\circ$. It can be assumed that standard enthalpy (ΔH°) and standard entropy (ΔS°) values are related, respectively, to the changes in intermolecular bond energies and to the rearrangements undergone by water molecules occurring during the binding. It has been verified that in various membrane receptors, agonist and antagonist behaviour can be distinguished *in vitro* on the basis of thermodynamic parameters of the binding equilibrium. In particular the binding of agonists may be entropy-driven and that of antagonists enthalpy-driven, or *vice versa*. Such a phenomenon has been defined ''thermodynamic discrimination'' and has been reported for β-adrenergic [1], glycine [2], GABA-A [3], serotonin 5-HT3 [4], nicotinic [5] and adenosine A_1, A_{2A} and A_3 adenosine receptors [6–9].

Adenosine is an endogenous nucleoside that modulates a number of physiological responses in all mammalian tissues by binding to specific G-protein-associated A_1, A_{2A}, A_{2B} and A_3 cell surface receptors. The A_1 and A_3 receptors are coupled to G_i protein and cause inhibition of adenylate cyclase (AC), whereas A_{2A} and A_{2B} receptor subtypes are coupled to G_s protein and cause an increase in AC activity. Adenosine receptors can also activate K^+ and inactivate Ca^{2+} channels, affect the activity of phospholipases C, D, A_2, regulate mitogen-activated protein kinases and inflammatory cytokines [10]. Adenosine levels increase under hypoxic, ischemic or inflamed conditions and play a critical role in cardioprotection, tissue protection and in the modulation of inflammatory processes. In addition the wide and abundant distribution of adenosine receptors suggests that they may be potentially useful therapeutic targets for drug development [11–13].

In particular the A_{2B} is a low affinity adenosine receptor that is highly expressed in the gastrointestinal tract, urinary bladder, lung tissue and in different immune cells [12]. A number of studies in literature demonstrated that it plays a proinflammatory role by stimulating the release of several inflammatory cytokines from mast cells, monocytes, airway epithelial cells, fibroblasts, smooth muscle cells and intestinal epithelial cells [14–18]. Indeed various A_{2B} antagonists are in development as anti-asthmatic drugs and are also of potential value as antidiabetic, antidiarrheal, and for cardiovascular disorders. Otherwise recent papers on A_{2B} knock-out mice suggested that this subtype may have also anti-inflammatory effects suggesting an enigmatic role for A_{2B} receptors in inflammatory diseases [19,20].

In spite of the strong relevance emerged in the last 10 years about the therapeutic role of the A_{2B} receptor, it is the only adenosine subtype that has not been studied yet from a thermodynamic point of view. Therefore with the aim of contributing to an evaluation of the molecular mechanisms underlying ligand–receptor interactions, that are important for drug development, this paper reports the results derived from the study of binding thermodynamics of six agonists and six antagonists to human A_{2B} receptors transfected in HEK 293 cells (hHEK293-A_{2B}). The results are compared with those obtained for the related A_1, A_{2A} and A_3 receptors, providing useful information on the binding mechanisms of all adenosine receptor subtypes.

2. Materials and methods

2.1. Materials

[^{3}H]MRE 2029-F20 (specific activity 123 Ci/mmol) was synthesized at Amersham International (Buckinghamshire, UK); CHA, NECA, R-PIA, S-PIA, CGS 15943, ZM 241385, DPCPX were obtained from Research Biochemical International (Natick, MA, USA). MRE 2029-F20, Compounds 17b, 21b, 24 and 34 were synthesized by Prof. P.G. Baraldi (Department of Pharmaceutical Sciences, University of Ferrara, Italy) [21,22]. All other reagents were of analytical grade and obtained from commercial sources.

2.2. Stable transfection of HEK 293 cells

HEK 293 cells were transfected with cDNA encoding human A_{2B} receptors as recently described [23] by using the calcium phosphate precipitation method [24]. Colonies were selected by growth of cells on 0.8 mg/ml G-418. Stably transfected cells were maintained in Dulbecco's modified Eagle's medium/Ham's F12 medium (DMEM/F12 medium) with 10% fetal calf serum, 100 U/ml penicillin, 100 mg/ml streptomycin and 0.3 mg/ml G-418, at 37° in 5% CO_2/95% air.

2.3. Membrane preparation

For membrane preparations the culture medium of hHEK293-A_{2B} cells was removed. The cells were washed with phosphate buffered saline (PBS) and scraped off T75 flasks in ice-cold hypotonic buffer (5 mM Tris–HCl, 2 mM EDTA, pH 7.4). The cell suspension was homogenized using a Polytron and the homogenate was spun for 30 min at 36,000 × *g*. The membrane pellet was resuspended in 50 mM Tris–HCl buffer, containing 10 mM $MgCl_2$, 1 mM EDTA, 0.1 mM benzamidine, pH 7.4 and incubated with 2 UI/ml of adenosine deaminase for 30 min at 37 °C. The protein concentration was determined according to a Bio-Rad method [25] with bovine albumin as reference standard.

2.4. [^{3}H]MRE 2029-F20 binding assays

Saturation binding experiments of [^{3}H]MRE 2029-F20 to hA_{2B} HEK293 cell membranes were performed at 4, 10, 15, 20, 25 and 30 °C in a thermostatic bath assuring a temperature of ±0.1 °C. All buffer solutions were adjusted to maintain a constant pH of 7.4 at the desired temperature. Competition experiments of 3 nM [^{3}H]MRE 2029-F20 were performed in duplicate in a final volume of 250 μl in test tubes containing 50 mM Tris–HCl buffer, 10 mM $MgCl_2$, 1 mM EDTA, 0.1 mM benzamidine pH 7.4, 100 μl of membranes and at least 12–14 different concentrations of typical adenosine receptor agonists and antagonists.

Table 1 – Affinities, expressed as K_D (nM) for [^{3}H]MRE 2029-F20 derived from saturation experiments to human A_{2B} transfected in HEK293 cells or K_i (nM) for selected adenosine receptor agonists and antagonists obtained by displacement of 3 nM [^{3}H]MRE 2029-F20 from the same receptors

Ligand	T (K)					
	277.15	283.15	288.15	293.15	298.15	303.15
Agonists						
Compound 24	64 ± 8	53 ± 7	46 ± 5	41 ± 6	36 ± 5	25 ± 4
Compound 34	88 ± 10	75 ± 8	70 ± 8	65 ± 7	58 ± 6	37 ± 5
NECA	283 ± 24	255 ± 22	230 ± 21	210 ± 18	202 ± 18	190 ± 20
R-PIA	3900 ± 365	3750 ± 352	3460 ± 341	3300 ± 335	3120 ± 315	3002 ± 308
S-PIA	8850 ± 890	7700 ± 690	7350 ± 675	7290 ± 650	7000 ± 680	6450 ± 610
CHA	4450 ± 430	4100 ± 400	4010 ± 390	3900 ± 380	3750 ± 350	3100 ± 300
Antagonists						
[^{3}H]MRE 2029-F20	2.8 ± 0.2	3.2 ± 0.3	3.7 ± 0.4	3.9 ± 0.4	5.2 ± 0.5	5.9 ± 0.5
ZM 241385	9 ± 1	14 ± 1	20 ± 2	26 ± 2	32 ± 3	40 ± 3
CGS 15943	11 ± 1	20 ± 2	26 ± 3	32 ± 3	40 ± 4	50 ± 4
DPCPX	35 ± 3	42 ± 4	53 ± 4	65 ± 5	87 ± 6	95 ± 8
Compound 17b	14 ± 2	20 ± 3	24 ± 3	30 ± 4	38 ± 5	45 ± 6
Compound 21b	19 ± 3	28 ± 3	35 ± 4	43 ± 5	51 ± 6	60 ± 7

Values are the mean ± S.E.M. of four separate experiments performed in triplicate.

Non-specific binding was defined as binding in the presence of 1 μM MRE 2029-F20 and, at the K_D value of the radioligand, was about 30–35% of total binding in HEK 293 cells. Similar results were obtained in the presence of 1 μM ZM 241385 and 100 μM NECA. Bound and free radioactivities were separated by filtering the assay mixture through Whatman GF/B glass-fiber filters using a Micro-Mate 196 cell harvester (Packard Instrument Company). The filter bound radioactivity was counted with a Top Count Microplate Scintillation Counter (efficiency 57%) with Micro-Scint 20. The protein concentration was determined according to a Bio-Rad method with bovine albumin as a standard reference. Incubation time ranged from 90 min at 4 °C to 60 min at 30 °C according to the results of previous time-course experiments. K_i values were calculated from IC_{50} values according to Cheng and Prusoff equation $K_i = IC_{50}/(1 + [C^*]/K_D^*)$, where $[C^*]$ is the concentration of the radioligand and K_D^* its dissociation constant. A weighted non-linear least-squares curve fitting program LIGAND [26] was used for computer analysis of saturation and inhibition experiments.

2.5. *Thermodynamic data calculation*

Evaluation of ΔG°, ΔH° and ΔS° values has been obtained by measurements of K_A (equilibrium association constant) carried out at different temperatures, followed by van't Hoff analysis. Two cases are to be distinguished: (1) the standard specific heat difference of the equilibrium (ΔC_p°) is essentially zero. In this case, the van't Hoff equation $\ln K_A = -\Delta H^\circ/RT + \Delta S^\circ/R$ gives a linear plot $\ln K_A$ versus $1/T$. The standard free energy can be calculated as $\Delta G^\circ = -RT \ln K_A$ at 298.15 K; the standard enthalpy (ΔH°) and the standard entropy (ΔS°) can be obtained from the slope ($-\Delta H^\circ/R$) and the intercept ($\Delta S^\circ/R$) of the van't Hoff plot $\ln K_A$ versus $1/T$, respectively, with $R = 8.314\ J\ K^{-1}\ mol^{-1}$. The linearity of the van't Hoff plot is not common in reactions involving biomacromolecules in solution but appears to be typical as far as membrane receptor binding is concerned. (2) ΔC_p° is different from zero: in this case the plot ΔG° versus T is often parabolic and other mathematical methods [27] for calculating the thermodynamic parameters of the equilibrium are available.

In the present case the van't Hoff plots can be considered to be essentially linear and the first method was applied.

3. Results

3.1. *Agonists and antagonists at A_{2B} adenosine receptors are therefore thermodynamically discriminated*

Table 1 reports the dissociation binding constants (K_D) values derived from the saturation experiments of [^{3}H]MRE 2029-F20 performed at the six chosen temperatures; the K_D values for the other selected ligands, measured as inhibitory binding constants (K_i) for the displacement of [^{3}H]MRE 2029-F20 in the same range of temperature are also reported. While K_D and K_i values changed with temperature, B_{MAX} values appear to be largely independent suggesting a same population of receptors at all temperatures, with a range of 420–450 fmol/mg of protein at the temperatures investigated. Fig. 1 shows the representative Scatchard plots obtained at the six temperatures investigated for the saturation equilibrium of [^{3}H]MRE 2029-F20. The plots are essentially linear at all the temperatures investigated and computer analysis of the data failed to show a significantly better fit to a two-site than to a one-site binding model, indicating that only one class of high affinity binding sites is present under our experimental conditions. Similar conclusions can be drawn from the analysis of the displacement curves concerning all other compounds in Table 1. The temperature dependence of the affinity constants $K_A = 1/K_i$, is shown in the van't Hoff plots, $\ln K_A$ versus $1/T$ of Figs. 2 and 3, which report the results for the six agonists and the six antagonists investigated, respectively. van't Hoff plots appear to be linear for all compounds in the complete range of temperature (4–30 °C).

Fig. 4 summarizes the results in the form of a $-T\Delta S^\circ$ versus ΔH° scatter plot ($T = 298.15$ K). It becomes apparent that all

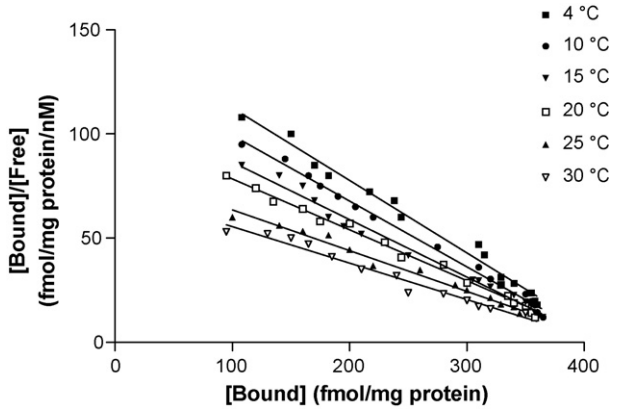

Fig. 1 – Representative Scatchard plots for [^{3}H]MRE 2029-F20 binding to hA_{2B} HEK293 cells at 4, 10, 15, 20, 25, 30 °C. The linearity of the plots is indicative of the presence of a single class of high affinity binding sites at all temperatures investigated.

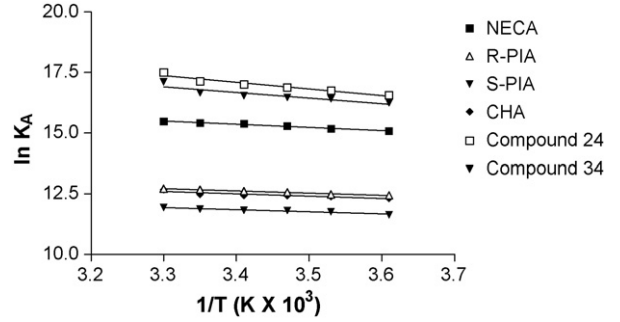

Fig. 2 – van't Hoff plots showing the effect of temperature on the equilibrium binding association constants, K_A, for six adenosine A_{2B} receptor agonists studied. All plots are essentially linear (*r* in the range 0.91–0.99) in the temperature range of 4–30 °C.

points are arranged on the same diagonal band encompassed between the two dashed lines which represent the loci of points defined by the limiting K_D values of 100 μM and 100 pM. This band is the expression of the enthalpy–entropy (*E–E*) compensation phenomenon [28]. Final thermodynamic parameters of the different compounds investigated are reported in Table 2. ΔG° values range from −42.5 to −29.3 kJ mol^{-1} for agonists and from −47.2 to −40.3 kJ mol^{-1} for antagonists. Equilibrium standard enthalpy (ΔH°) and entropy (ΔS°) values show that the binding of agonists is always totally entropy-driven while is enthalpy and entropy-driven for antagonists, ΔH° values ranging from 7 to 23 and from −40 to −20 kJ mol^{-1} and ΔS° values from 123 to 219 and from 10 to 91 J (K mol)$^{-1}$ for agonists and antagonists, respectively. Agonists and antagonists are therefore thermodynamically discriminated.

4. Discussion

In the field of adenosine receptors, binding thermodynamic analysis has been performed until now at A_1, A_{2A} and A_3 adenosine subtypes. The only subtype lacking of this analysis was the A_{2B} for which, until few years ago, no high affinity radioligands were available. Previously we have characterized A_{2B} adenosine receptors in stably transfected HEK 293 cells by using the selective antagonist [^{3}H]MRE 2029-F20 [23]. Therefore with the aim to obtain new information concerning molecular mechanisms underlying ligand–receptor interactions, in this study, we have determined the thermodynamic parameters related to the binding of 12 ligands (six agonists and six antagonists) at human A_{2B} adenosine receptors. The most relevant results of this study concern the thermodynamic discrimination of agonists from antagonists and the recurrent phenomenon of *E–E* compensation.

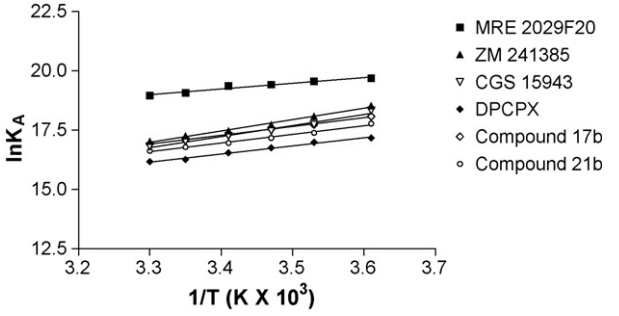

Fig. 3 – van't Hoff plots showing the effect of temperature on the equilibrium binding association constants, K_A, for six adenosine A_{2B} receptor antagonists studied. All plots are essentially linear (*r* in the range 0.98–0.99) in the temperature range of 4–30 °C.

All compounds studied display essentially linear van't Hoff plots indicating that the ΔC_p° (standard specific heat difference of the equilibrium) values of the drug–receptor binding equilibrium is nearly zero or, in other words, that ΔH° values

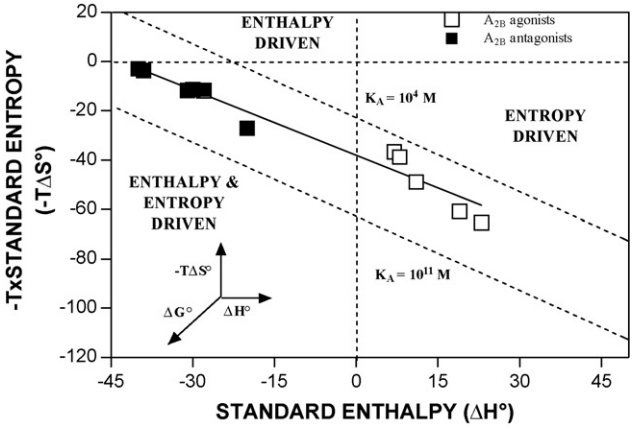

Fig. 4 – Scatter plot of $-T\Delta S^\circ$ vs. ΔH° values for the adenosine A_{2B} receptor ligands studied. Full and open symbols indicate antagonists and agonists, respectively. All points lie on a same regression line. The two dashed lines indicate the loci of the points representing possible combinations of ΔH° and $-T\Delta S^\circ$ values giving rise to the two different equilibrium constants indicated ($K_A = 10^4$ and $K_A = 10^{11}$).

Table 2 – Thermodynamic parameters for displacement of [^{3}H]MRE 2029-F20, by adenosine agonists and antagonists from human A_{2B} cloned receptors expressed in HEK 293 cells

Ligand	ΔG° (kJ mol^{-1})	ΔH° (kJ mol^{-1})	ΔS° (J K^{-1} mol^{-1})
Agonists			
Compound 24	−42.5 ± 0.2	23 ± 2	219 ± 9
Compound 34	−41.4 ± 0.2	19 ± 2	204 ± 10
NECA	−38.0 ± 0.2	11 ± 1	164 ± 5
R-PIA	−31.3 ± 0.1	8 ± 1	130 ± 5
S-PIA	−29.3 ± 0.1	7 ± 1	123 ± 4
CHA	−31.0 ± 0.1	8 ± 1	130 ± 6
Antagonists			
[^{3}H]MRE 2029-F20	−47.2 ± 0.2	−20 ± 2	91 ± 6
ZM 241385	−42.5 ± 0.1	−40 ± 4	10 ± 1
CGS 15943	−42.0 ± 0.2	−39 ± 3	12 ± 1
DPCPX	−40.3 ± 0.1	−28 ± 3	40 ± 2
Compound 17b	−42.2 ± 0.1	−31 ± 3	39 ± 2
Compound 21b	−41.4 ± 0.1	−30 ± 3	38 ± 2

Equilibrium ΔG°, ΔH° and ΔS° values are given at T = 298.15 K.

are not significantly affected by temperature in the range investigated (4–30 °C). Such linearity appears to be a typical property of the drug–membrane receptor binding [28], unlike most binding processes between molecules and biomacromolecules occurring in solution [29].

Fig. 4 summarizes in the form of a $-T\Delta S^\circ$ versus ΔH° plot the results of the thermodynamic measurements given in Table 2. All the compounds investigated appear to be arranged along a same diagonal line, according to the equation $-T\Delta S^\circ$ (kJ mol^{-1} at 298.15 K) = −38 (±2) − 0.88 (±0.04) ΔH° (kJ mol^{-1}) (n = 12, r = −0.974, $P < 0.0001$). This equation can be rewritten as $\Delta H^\circ = \beta\ \Delta S^\circ$, which is the form for a case of enthalpy-entropy compensation [28,30] with a compensation temperature of 320 °K. This phenomenon seems to be a common feature in all cases of drug–receptor binding [28] and its general implications have been discussed by different authors [30,31].

Recently, the enthalpy–entropy compensation phenomenon has been attributed, for drug–receptor interactions, to the solvent reorganisation that accompanies the receptor binding process in diluted solutions [30]. According to this point of view, while ΔG° values are most probably determined by the features of the ligand–receptor binding process, ΔH° and $-T\Delta S^\circ$ values appear strongly affected by the rearrangements occurring in the solvent [30]. Finally, we observed that the binding equilibrium of A_{2B} receptor ligands is entropy-driven for agonists, but mostly enthalpy-driven for antagonists. In fact the plot of $-T\Delta S^\circ$ versus ΔH° indicates that agonists cluster in a region of endothermicity and entropy increase, while antagonists gather together in a different cluster of exothermicity and less favoured entropy change. Accordingly, agonists and antagonists are thermodynamically discriminated for all adenosine receptors studied so far [6–9]. An overall analysis of thermodynamic data for representative adenosine agonists and antagonists at A_1, A_{2A}, A_{2B} and A_3 adenosine receptors is reported in Fig. 5 and Tables 3A and 3B; the correlation equation of the $-T\Delta S^\circ$ versus ΔH° scatter plot is: $-T\Delta S^\circ$ (kJ mol^{-1} at 298.15 K) = −41.39 (±0.9) − 1.02 (±0.04) ΔH° (kJ mol^{-1}) (n = 47, r = −0.97, $P < 0.0001$) suggesting that the ΔH° and $-T\Delta S^\circ$ of the single adenosine subtypes are independently correlated on the same straight line. In this light we suggest that the similarity in thermodynamic parameters probably reflects a common mechanism of ligand–receptor interaction for all adenosine receptors subtypes and this may explain the difficulty to obtain selective adenosine ligands. However the development of therapeutic substances has been strongly advanced by rational drug design, which involves achieving full understanding of a given biomolecular interaction by combining structural, kinetic and thermodynamic information [32–35]. Therefore, the availability of thermodynamic data adds important information to the decision-making process in drug development [36,37]. In particular, when compounds have similar affinities, their enthalpy (ΔH) values can be used to select one as the preferred lead compound for optimisation. A favourable ΔH term implies better complementarity of the binding interfaces, because enthalpy corresponds to the energy associated with the net change in non-covalent bonds [36,37]. Some of the antagonists studied in this work such as MRE 2029-F20 are in preclinical phase as anti-asthmatic agents. Interestingly, a recent work by Vidal et al. [39] reports

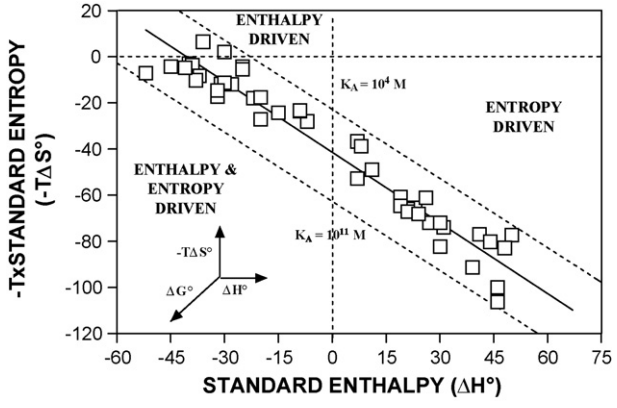

Fig. 5 – Scatter plot of $-T\Delta S^\circ$ vs. ΔH° values for representative adenosine receptor ligands at A_1, A_{2A}, A_{2B} and A_3 adenosine receptors. All points lie on a same regression line. The two dashed lines indicate the *loci* of the points representing possible combinations of ΔH° and $-T\Delta S^\circ$ values giving rise to the two different equilibrium constants indicated ($K_A = 10^4$ and $K_A = 10^{11}$).

Table 3A – Binding thermodynamic parameters of adenosine agonists at A_1, A_{2A}, A_{2B} and A_3 adenosine receptors included in Fig. 5 (ΔG°, ΔH° and ΔS° values are given at T = 298.15 K)

Agonists	ΔG° (kJ mol^{-1})	ΔH° (kJ mol^{-1})	ΔS° (J (K mol)$^{-1}$)	References
A_1 receptors				
CHA	−51.1 ± 0.2	39 ± 5	306 ± 17	[7]
CPA	−59.9 ± 0.3	46 ± 7	356 ± 24	[7]
R-PIA	−52.0 ± 0.3	30 ± 8	276 ± 28	[7]
S-PIA	−45.1 ± 0.1	21 ± 1	221 ± 5	[7]
NECA	−46.0 ± 0.1	19 ± 1	217 ± 5	[7]
CGS 21680	−34.7 ± 0.3	26 ± 6	205 ± 21	[8]
A_{2A} receptors				
CGS 21680	−44.9 ± 0.1	27 ± 3	241 ± 9	[8]
NECA	−45.8 ± 0.2	7 ± 5	177 ± 19	[8]
R-PIA	−35.3 ± 0.1	41 ± 6	258 ± 20	[8]
S-PIA	−27.2 ± 0.1	50 ± 5	259 ± 18	[8]
CPA	−36.2 ± 0.2	44 ± 5	269 ± 18	[8]
CHA	−34.9 ± 0.3	48 ± 7	278 ± 23	[8]
A_{2B} receptors				
Compound 24	−42.5 ± 0.2	23 ± 2	219 ± 9	Present work
Compound 34	−41.4 ± 0.2	19 ± 2	204 ± 10	Present work
NECA	−38.0 ± 0.2	11 ± 1	164 ± 5	Present work
R-PIA	−31.3 ± 0.1	8 ± 1	130 ± 5	Present work
S-PIA	−29.3 ± 0.1	7 ± 1	123 ± 4	Present work
CHA	−31.0 ± 0.1	8 ± 1	130 ± 6	Present work
A_3 receptors				
IB-MECA	−55.2 ± 0.2	67 ± 5	410 ± 8	[9]
Cl-IB-MECA	−53.8 ± 0.1	46 ± 3	335 ± 5	[9]
AB-MECA	−46.6 ± 0.2	21 ± 1	225 ± 4	[9]
NECA	−44.3 ± 0.1	24 ± 2	228 ± 9	[9]
R-PIA	−43.1 ± 0.2	31 ± 2	248 ± 7	[9]
S-PIA	−41.3 ± 0.3	30 ± 1	241 ± 5	[9]

Table 3B – Binding thermodynamic parameters of adenosine antagonists at A_1, A_{2A}, A_{2B} and A_3 adenosine receptors included in Fig. 5 (ΔG°, ΔH° and ΔS° values are given at T = 298.15 K)

Antagonists	ΔG° (kJ mol^{-1})	ΔH° (kJ mol^{-1})	ΔS° (J K^{-1} mol^{-1})	References
A_1 receptors				
DPCPX	−49.2 ± 0.1	−32 ± 1	58 ± 4	[7]
CPT	−45.1 ± 0.2	−37 ± 4	28 ± 14	[7]
8-PT	−40.2 ± 0.1	−22 ± 1	60 ± 4	[7]
DPSPX	−38.0 ± 0.1	−20 ± 2	59 ± 6	[7]
IBMX	−30.1 ± 0.3	−36 ± 9	−22 ± 33	[7]
Theophylline	−28.2 ± 0.2	−30 ± 5	−7 ± 19	[7]
A_{2A} receptors				
DPCPX	−35 ± 0.2	−7 ± 5	94 ± 18	[8]
SCH 58261	−49.0	−45	14	[38]
SCH 63390	−46.5	−32	49	[38]
8-PT	−32.6 ± 0.1	−9 ± 2	79 ± 10	[8]
Theophylline	−29.5 ± 0.1	−25 ± 3	14 ± 11	[8]
IBMX	−30.4 ± 0.1	−25 ± 3	18 ± 9	[8]
A_{2B} receptors				
MRE 2029-F20	−47.2 ± 0.2	−20 ± 2	91 ± 6	Present work
ZM 241385	−42.5 ± 0.1	−40 ± 4	10 ± 1	Present work
CGS 15943	−42.0 ± 0.2	−39 ± 3	12 ± 1	Present work
DPCPX	−40.3 ± 0.1	−28 ± 3	40 ± 2	Present work
Compound 17b	−42.2 ± 0.1	−31 ± 3	39 ± 2	Present work
Compound 21b	−41.4 ± 0.1	−30 ± 3	38 ± 2	Present work
A_3 receptors				
MRE 3008-F20	−48.7 ± 0.2	−38 ± 1	34 ± 4	[9]
MRE 3020-F20	−46.2 ± 0.1	−41 ± 2	16 ± 2	[9]
MRE 3005-F20	−44.8 ± 0.2	−52 ± 2	24 ± 2	[9]
CGS 15943	−39.6 ± 0.1	−15 ± 1	81 ± 6	[9]
DPCPX	−32.6 ± 0.2	−9 ± 1	78 ± 8	[9]

the discovery and characterization of a novel potent, selective and efficacious A_{2B} antagonist (LAS38096). This compound showed efficacy in functional *in vitro* and *in vivo* models of allergy and inflammation further suggesting that blockade of the A_{2B} receptor may provide clinical benefits in the treatment of chronic respiratory diseases [39].

REFERENCES

[1] Weiland GA, Minneman KP, Molinoff PB. Fundamental difference between the molecular interactions of agonists and antagonists with the beta-adrenergic receptor. Nature 1979;281:114–7.
[2] Gomez AR, Garcia Calvo M, Vasquez J, Marvizon CG, Valdiviero T, Major F. Thermodynamics of agonist and antagonist interaction with the strychnine-sensitive glycine receptor. J Neurochem 1989;52:1775–80.
[3] Maksay G. Thermodynamics of gamma-aminobutyric acid type A receptor binding differentiate agonists from antagonists. Mol Pharmacol 1994;46:386–90.
[4] Borea PA, Dalpiaz A, Gessi S, Gilli G. Thermodynamics of 5-HT3 receptor binding discriminates agonistic from antagonistic behaviour. Eur J Pharmacol 1996;298: 329–34.
[5] Borea PA, Varani K, Gessi S, Gilli P, Gilli G. Binding thermodynamics at the human neuronal nicotine receptor. Biochem Pharmacol 1998;55:1189–97.
[6] Dalpiaz A, Townsend-Nicholson A, Beukers MW, Schofield PR, IJzerman AP. Thermodynamics of full agonist, partial agonist, and antagonist binding to wild-type and mutant adenosine A_1 receptors. Biochem Pharmacol 1998;56:1437–45.
[7] Borea PA, Varani K, Guerra L, Gilli P, Gilli G. Binding thermodynamics of A_1 adenosine receptor ligands. Mol Neuropharmacol 1992;2:273–81.
[8] Borea PA, Dalpiaz A, Varani K, Guerra L, Gilli G. Binding thermodynamics of adenosine A_{2A} receptor ligands. Biochem Pharmacol 1995;49:461–9.
[9] Merighi S, Varani K, Gessi S, Klotz K-N, Leung E, Baraldi PG, et al. Binding thermodynamics at the human A_3 adenosine receptor. Biochem Pharmacol 2002;63:157–61.
[10] Fredholm BB, Ijzerman AP, Jacobson KA, Klotz KN, Linden J. International union of pharmacology. XXV. Nomenclature and classification of adenosine receptors. Pharmacol Rev 2001;53:527–52.
[11] Holgate ST. The identification of the adenosine A_{2B} receptor as a novel therapeutic target in asthma. Br J Pharmacol 2005;145:1009–15.
[12] Jacobson KA, Gao ZG. Adenosine receptors as therapeutic targets. Nat Rev Drug Discov 2006;5:247–64.
[13] Fredholm BB. Adenosine receptors as targets for drug development. Drug News Perspect 2003;16:283–9.
[14] Feoktistov I, Biaggioni I. Adenosine A_{2B} receptors evoke interleukin-8 secretion in human mast cells. J Clin Invest 1995;96:1979–86.
[15] Ryzhov S, Goldstein AE, Biaggioni I, Feoktistov I. Cross-talk between Gs and Gq-coupled pathways in regulation of interleukin-4 by A_{2B} adenosine receptors in human mast cells. Mol Pharmacol 2006;70:727–35.
[16] Zhong H, Belardinelli L, Maa T, Feoktistov I, Biaggioni I, Zeng D. A_{2B} adenosine receptors increase cytokine release by bronchial smooth muscle cells. Am J Respir Cell Mol Biol 2004;30:118–25.
[17] Sun C-X, Zhong H, Mohsenin A, Morschi E, Chung JL, Molina JG, et al. Role of A_{2B} adenosine receptor signalling in adenosine-dependent pulmonary inflammation and injury. J Clin Invest 2006;116:2173–82.
[18] Strohmeier GR, Reppert SM, Lencer WI, Madara JL. The A_{2B} adenosine receptor mediates cAMP responses to adenosine receptor agonists in human intestinal epithelia. J Biol Chem 1995;270:2387–94.
[19] Yang D, Zhang Y, Nguyen HG, Koupenova M, Chauhan AK, Makitalo M, et al. The A_{2B} adenosine receptor protects against inflammation and excessive vascular adhesion. J Clin Invest 2006;116:1913–23.
[20] Hua X, Kovarova M, Chason KD, Nguyen M, Koller BH, Tilley SL. Enhanced mast cell activation in mice deficient in the A_{2B} adenosine receptor. J Exp Med 2007;204:117–28.
[21] Baraldi PG, Tabrizi MA, Preti D, Bovero A, Romagnoli R, Fruttarolo F, et al. Design, synthesis, and biological evaluation of new 8-heterocyclic xanthine derivatives as highly potent and selective human A_{2B} adenosine receptor antagonists. J Med Chem 2004;47:1434–47.
[22] Baraldi PG, Preti D, Tabrizi MA, Fruttarolo F, Saponaro G, Baraldi S, et al. N^6-[(Hetero)aryl/(cyclo)alkyl-carbamoyl-methoxy-phenyl]-(2-chloro)-5′-N-ethylcarboxamido-adenosines: the first example of adenosine-related structures with potent agonist activity at the human A_{2B} adenosine receptor. Bioorg Med Chem 2007;15:2514–27.
[23] Gessi S, Varani K, Merighi S, Cattabriga E, Pancaldi C, Szabadkai Y, et al. Expression, pharmacological profile and functional coupling of A_{2B} receptors in a recombinant system and in peripheral blood cells by using a novel selective antagonist radioligand [^{3}H]MRE 2029F20. Mol Pharmacol 2005;67:2137–47.
[24] Chen C, Okaiama H. High-efficiency transformation of mammalian cells by plasmid DNA. Mol Cell Biol 1987;7:2745–52.
[25] Bradford MM. A rapid and sensitive method for the quantification of microgram quantities of protein utilizing the principle of protein dye-binding. Anal Biochem 1976;72:248–54.
[26] Munson PJ, Rodbard D. Ligand: a versatile computerized approach for the characterization of ligand binding systems. Anal Biochem 1980;107:220–39.
[27] Osborne JP, Palumbo G, Brewer HB, Edelhoch H. The thermodynamics of the self-association of the reduced and carboxymethylated form of Apo A-II from the human high density lipoprotein complex. Biochemistry 1976;15:317–20.
[28] Gilli P, Ferretti V, Gilli G, Borea PA. Enthalpy-entropy compensation in drug-receptor binding. J Phys Chem 1994;98:1515–8.
[29] Sturtevant JM. Heat capacity and entropy changes in processes involving proteins. Proc Natl Acad Sci USA 1977;74:2236.
[30] Tomlinson E. Enthalpy-entropy compensation analysis of pharmaceutical, biochemical and biological systems. Int J Pharmaceutics 1983;13:115–44.
[31] Grunwald E, Steel C. Solvent reorganization and thermodynamic enthalpy-entropy compensation. J Am Chem Soc 1995;117:5687–92.
[32] Holdgate GA, Ward WHJ. Measurements of binding thermodynamics in drug discovery. Drug Discov Today 2005;10:1543–50.
[33] Whitesides GM, Krishnamurthy VM. Designing ligands to bind proteins. Q Rev Biophys 2006;38:385–95.
[34] Testa B, Jenner P, Kilpatrick GJ, El Tayar N, van de Waterbeemd H, Marsden CD. Do thermodynamic studies provide information on both the binding to and the activation of dopaminergic and other receptors? Biochem Pharmacol 1987;36:4041–6.
[35] Raffa RB, Porreca F. Thermodynamic analysis of the drug-receptor interaction. Life Sci 1989;44:245–58.

[36] Ladbury JE. Application of isothermal titration calorimetry in the biological sciences: things are heating up! Biotechniques 2004;37:885–7.
[37] Moll D, Schweinsberg S, Hammann C, Herberg FW. Comparative thermodynamic analysis of cyclic nucleotide binding to protein kinase A. Biol Chem 2007;388:163–72.
[38] Baraldi PG, Cacciari B, Spalluto G, Bergonzoni M, Dionisotti S, Ongini E, et al. Design, synthesis and biological evaluation of a second generation of pyrazolo[4,3-e]-1,2,4-triazolo[1,5-c]pyrimidines as potent and selective A_{2A} adenosine receptor antagonists. J Med Chem 1998;41:2126–33.
[39] Vidal B, Nueda A, Esteve C, Domenech T, Benito S, reinoso RF, et al. Discovery and characterization of 4′-(2-Furyl)-N-pyridin-3-yl-4,5′-bipyrimidin-2′-amine (LAS38096), a potent selective, and efficacious A_{2B} adenosine receptor antagonist. J Med Chem 2007;50:2732–6.